

MICROBEAMS WITH SURFACE AND PIEZOELECTRIC EFFECTS IN AFM

JULIO R. CLAEYSSSEN*, LETICIA TONETTO[†], TERESA TSUKAZAN[‡]

**Institute of Mathematics, UFRGS
Av. Bento Gonçalves, 9500, 91509-900,
Porto Alegre, Rio Grande do Sul, Brazil*

*[†]Program of Applied Mathematics, UFRGS
Av. Bento Gonçalves, 9500, 91509-900,
Porto Alegre, Rio Grande do Sul, Brazil*

*[‡]Institute of Mathematics, UFRGS
Av. Bento Gonçalves, 9500, 91509-900,
Porto Alegre, Rio Grande do Sul, Brazil*

Emails: julio@mat.ufrgs.br, ltonetto.mat@gmail.com, teresa@mat.ufrgs.br

Abstract— Microbeam models with surface and piezoelectric effects are considered for atomic force microscopy (AFM). These models include rotatory inertia and shear deformation as proposed by Timoshenko and they are subject to forcing loads. Eigenanalysis of the free dynamic matrix model is performed with the use of a fundamental matrix response to determine the modal frequency equation and matrix mode shapes. The fundamental response governs the behaviour of a non-classical damped second-order matrix differential equation. It was observed that surface effects are influential for the natural frequency at the nanoscale. When the beam length increases from nanometers to microns, the surface effects disappear and the results converge into natural frequencies of classical Timoshenko model. Simulations with the piezoelectric model were performed to observe the effects of forcing pulses located at different positions of the microbeam.

Keywords— Dynamic of nanomaterials, Atomic force microscopy, surface and piezoelectric effects, Timoshenko beam model.

1 Introduction

In this work, transversal vibrations of interest in atomic force microscopy (AFM) are discussed with a microbeam subject to surface effects and built with smart materials. The motion of the microbeam is governed by the Timoshenko model. The surface effects are observed when downsizing from the micron scale to the nanoscale. The action of piezoelectric materials in the role of actuators and/or sensors are considered through pulse forcing at different locations of the microbeam.

A typical AFM consists of a sensitive microcantilever with a mounted sharp tip acting as force sensor, a system that moves the sample or the sensor in order to probe the sample surface, a detection sensor system of the cantilever deflection, a feedback system which regulates the force interaction and an electronic controller system which records movements, controls the feedback loop and sends the measured data to a computer processing unit. The geometry and the material of the cantilever both contribute to the properties that make a cantilever suitable for any particular imaging modes. Both silicon and silicon nitride microcantilevers are commercially available but reflective back surface coating is used for a better feedback. New generations of nanobeams have included piezoelectric materials locally attached at the microbeam with the role of sensors and/or actuators (Jalili, 2010), (Laxminarayana and Jalili, 2004), (Eslami and Jalili, 2012).

The use of the AFM, as nanomachining or as a platform for chemical and biological sensors in connection with surface and thermal effects, make that the effects of transverse shear deformation and rotary inertia on the frequency be significant. Furthermore, to model a thick beam with high frequency excitation, as usually occurs in micro-systems, the Timoshenko theory of beam must be employed. With smaller values of the ratio of the probe length to its thickness, the Timoshenko beam theory is able to predict the frequencies of flexural vibrations of the higher modes with higher stiffness for the AFM cantilevers (Hsu et al., 2007).

When the associated length scales are sufficiently small, the applicability of classical continuum models can not be appropriate. This topic have been discussed in the corresponding literature with proposed mathematical models that includes different effects, such as surface effects and non-local effects which modifies conventional beam theories for size dependent systems. When the characteristic sizes of materials and structures shrink to microns or nanometers, surface/tension effects must be taken into account because they play an significant role in their mechanical behavior due to the increasing ratio between surface/interface area and volume (Gurtin et al., 1998), (Abbasion et al., 2009).

The two models considered in this work are formulated as a second-order evolution system subject to initial, forcing and boundary data. The

distributed matrix impulse response or initial-value Green matrix response is used for characterizing transients and forced responses in AFM. The vibration modes can be explicitly formulated in terms of a fundamental matrix response of a second-order matrix ordinary differential equation where the corresponding stiffness matrix coefficient depends non linearly upon the frequency. This matrix response can be determined in closed form in terms of a scalar solution that has a completely oscillatory behavior beyond a critical frequency value (Claeysen et al., 1999), (Claeysen and Costa, 2006).

Simulations with surface effects were performed to observe the influence upon the natural frequency at nanoscale. For the piezoelectric model, pulse forcing effects were considered at different locations of the microbeam and observed that they are more sensed when closer to the tip-sample interaction.

2 Timoshenko beam with surface effects

We consider the microcantilever having length L , width b , thickness $2h$ and mass density area of the beam ρ . We let $I = \frac{2bh^3}{3}$ be the moment of inertia of the cross section area $A = 2bh$, $w(t, x)$ the flexural deflection of the beam, $\psi(t, x)$ the rotation angle of cross section of the beam, $f(t, x)$ a transverse dynamic load and $q(t, x)$ a moment load. The governing equations are given by (Abbasion et al., 2009),

$$\rho A w_{tt} - \kappa G A w_{xx} + \overline{\kappa G A} \psi_x = f(t, x), \quad (1)$$

$$\rho I \psi_{tt} - \overline{EI} \psi_{xx} - \kappa G A (w_x - \psi) = q(t, x),$$

where

$$\overline{\kappa G A} = \kappa G A - (\tau_u + \tau_b)b, \quad (2)$$

$$\overline{EI} = (EI + 2bh^2 E_s), \quad (3)$$

are the effective curvature effect and flexural rigidity, respectively. Here τ_u and τ_b denote the upper and lower surfaces residual tensions and E_s is a surface elastic modulus. The boundary conditions are those of a cantilever beam or subject to balance of the moment and shear at the free end $x = L$. The Young's modulus, shear modulus, mass density, shear deformation factor of the beam are denoted as E , G , ρ and κ , respectively.

2.1 Matrix formulation

The coupled Timoshenko model (1) can be written as a second-order differential equation with matrix coefficients

$$M\ddot{\mathbf{v}} + \mathbf{K}\mathbf{v} = \mathbf{F}, \quad (4)$$

where

$$\mathbf{v} = \begin{pmatrix} w(t, x) \\ \psi(t, x) \end{pmatrix}, \quad \mathbf{F} = \begin{pmatrix} f(t, x) \\ q(t, x) \end{pmatrix}, \quad (5)$$

$$\mathbf{M} = \begin{pmatrix} \rho A & 0 \\ 0 & \rho I \end{pmatrix}, \quad \mathbf{K} = \mathbf{E} \frac{\partial^2}{\partial x^2} + \mathbf{N} \frac{\partial}{\partial x} + \mathbf{R}, \quad (6)$$

with

$$\mathbf{E} = \begin{pmatrix} -\kappa G A & 0 \\ 0 & -\overline{EI} \end{pmatrix}, \quad \mathbf{N} = \begin{pmatrix} 0 & \overline{\kappa G A} \\ -\kappa G A & 0 \end{pmatrix},$$

$$\mathbf{R} = \begin{pmatrix} 0 & 0 \\ 0 & \kappa G A \end{pmatrix}.$$

For a microcantilever beam of length L , we have the boundary conditions in a matrix formulation

$$\begin{pmatrix} 1 & 0 \\ 0 & 1 \end{pmatrix} \mathbf{v}(t, 0) + \begin{pmatrix} 0 & 0 \\ 0 & 0 \end{pmatrix} \mathbf{v}_x(t, 0) = \mathbf{0}, \quad (7)$$

$$\begin{pmatrix} 0 & 0 \\ 0 & -1 \end{pmatrix} \mathbf{v}(t, L) + \begin{pmatrix} 0 & 1 \\ 1 & 0 \end{pmatrix} \mathbf{v}_x(t, L) = \mathbf{0},$$

or in a more compact form

$$\begin{aligned} \mathbf{A}\mathbf{v}(t, 0) + \mathbf{B}\mathbf{v}_x(t, 0) &= \mathbf{0}, \\ \mathbf{P}\mathbf{v}(t, L) + \mathbf{Q}\mathbf{v}_x(t, L) &= \mathbf{0}. \end{aligned} \quad (8)$$

2.2 Eigenanalysis

The search of exponential solutions

$$\mathbf{v}(t, x) = e^{\lambda t} \mathbf{v}(x), \quad \mathbf{v}(x) = \begin{pmatrix} w(x) \\ \psi(x) \end{pmatrix}, \quad (9)$$

of the unforced Timoshenko model

$$\mathbf{M} \frac{\partial^2 \mathbf{v}}{\partial t^2} + \mathbf{K} \mathbf{v} = \mathbf{0}, \quad (10)$$

subject to general separated homogeneous boundary conditions (8). And \mathbf{v} is the general solution of a second-order matrix differential equations and is given by (Claeysen et al., 1999)

$$\mathbf{v}(x) = \mathbf{h}(x) \mathbf{c}_1 + \mathbf{h}'(x) \mathbf{c}_2, \quad (11)$$

for constant 2×1 vectors \mathbf{c}_1 and \mathbf{c}_2 . Here $\mathbf{h}(x)$ is the 2×2 matrix solution of the initial value problem

$$\begin{aligned} \mathbf{M} \mathbf{h}''(x) + \mathbf{C} \mathbf{h}'(x) + \mathbf{K}(\lambda) \mathbf{h}(x) &= \mathbf{0}, \\ \mathbf{h}(0) &= \mathbf{0}, \quad \mathbf{M} \mathbf{h}'(0) = \mathbf{I}, \end{aligned} \quad (12)$$

where $\mathbf{0}$ denotes the 2×2 null matrix and \mathbf{I} the 2×2 identity matrix. The matrix coefficients

with

$$M = \begin{pmatrix} -\kappa GA & 0 \\ 0 & -\overline{EI} \end{pmatrix}, \quad C = \begin{pmatrix} 0 & \overline{\kappa GA} \\ -\kappa GA & 0 \end{pmatrix}, \quad \epsilon = \frac{1}{2} \sqrt{-2g^2 + 2\sqrt{g^4 + 4r^4}}, \quad (20)$$

$$K(\lambda) = \begin{pmatrix} \rho A \lambda^2 & 0 \\ 0 & \lambda^2 \rho I + \kappa GA \end{pmatrix}, \quad \delta = \frac{1}{2} \sqrt{2g^2 + 2\sqrt{g^4 + 4r^4}}. \quad (21)$$

and

$$\begin{aligned} a &= \kappa GA, & c &= \rho A, & e &= \rho I, \\ a_m &= \overline{\kappa GA} = \kappa GA - (\tau_u + \tau_b)b, \\ b_m &= \overline{EI} = (EI + 2bh^2 E_s). \end{aligned} \quad (22)$$

Since we have the clamped boundary condition $\mathbf{v}(0) = \mathbf{0}$, by using the initial values of $\mathbf{h}(x)$ in (11), it turns out that $\mathbf{c}_2 = \mathbf{0}$. Thus we have to determine λ so that

$$\mathbf{v}(x) = \mathbf{h}(x, \lambda) \mathbf{c}_1 \quad (13)$$

satisfies the boundary condition at the free end $x = L$. By assuming homogeneous boundary conditions, we have the nonlinear eigenmatrix problem

$$\mathbf{U}(\lambda) \mathbf{c} = (\mathbf{P} \mathbf{h}(\mathbf{L}, \lambda) + \mathbf{Q} \mathbf{h}'(\mathbf{L}, \lambda)) \mathbf{c}_1 = \mathbf{0}. \quad (14)$$

From this, it turns out the characteristic equation

$$\Delta(\lambda) = \det(\mathbf{U}) = 0. \quad (15)$$

We thus have the reduced system

$$\mathcal{U}_D \mathbf{c}_1 = \mathbf{0}, \quad \mathbf{c}_1 = \begin{pmatrix} c_{11} \\ c_{12} \end{pmatrix}^T, \quad (16)$$

with

$$\mathcal{U}_D = \begin{pmatrix} ad''(L) \\ -b_m d'''(L) + \lambda^2 ed'(L) \\ -ad'''(L) + \lambda^2 cd'(L) \\ ad''(L) - \lambda^2 cd(L) - a_m d''(L) \end{pmatrix}. \quad (17)$$

The natural frequencies $\lambda = i\omega$ can be obtained by substituting the roots of the characteristic equation

$$\Delta(\omega) = -\omega^4 ce (d'(L))^2 + \omega^2 [ac d(L) d''(L) - (ae + cb_m) d'(L) d'''(L)] + (a^2 - aa_m) (d''(L))^2 - ab_m (d'''(L))^2, \quad (18)$$

where

$$d(x) = \frac{\delta \sinh(\epsilon x) - \epsilon \sinh(\delta x)}{ab_m \epsilon \delta (\delta^2 + \epsilon^2)}, \quad (19)$$

is the solution of the initial value problem

$$\begin{aligned} ab_m d^{(iv)}(x) + (-ae\lambda^2 - c\lambda^2 b_m - a^2 + a_m a) d''(x) + \\ (c\lambda^2 a + c\lambda^4 e) d(x) = 0, \\ d(0) = d'(0) = d''(0) = 0, ab_m d'''(0) = 1, \end{aligned}$$

$$\begin{aligned} g^2 &= \overline{g_m^2} + \overline{s^2}, & \overline{g_m^2} &= -\left(\frac{e}{b_m} + \frac{c}{a}\right) \lambda^2, \\ \overline{s^2} &= \frac{1}{b_m} (a_m - a), & \overline{r^4} &= -c\lambda^2 \left(\frac{a+e\lambda^2}{ab_m}\right). \end{aligned} \quad (23)$$

The response $\mathbf{h}(x)$ is obtained in (Claeysen et al., 1999)

$$\mathbf{h}(x) = \begin{pmatrix} (a + e\lambda^2)d(x) - b_m d''(x) & -a_m d'(x), \\ ad'(x) & -ad''(x) + c\lambda^2 d(x), \end{pmatrix}.$$

For a microcantilever beam described by the Timoshenko model with surface effects, Figure 1 illustrates the size dependence in the natural frequency of Timoshenko classical model and Timoshenko model including surface effects. The solutions based on classical Timoshenko beam theory and Timoshenko beam theory including surface effects are denoted by TB and TMB, respectively. The fundamental natural frequencies are normalized to fundamental frequency of cantilever Euler-Bernoulli beam. In this figure are considered the parameters utilized in (Abbasion et al., 2009) for the same purposes. The parameters of surface elasticity and residual surface tension can be determined by molecule dynamics simulations or experiments. Residual surface stresses can be either positive or negative, depending on the crystallographic structure (Wang and Feng, 2007). For an anodic alumina *Al* (Young's modulus $E = 70 \text{ GPa}$, Poisson's ratio $\nu = 0.3$ and $\rho = 2700 \text{ kg/m}^3$) are considered two types of crystallographic direction

$$Al[100]: E_s = -7.9253 \text{ N/m and } \tau = 0.5689 \text{ N/m},$$

$$Al[111]: E_s = 5.1882 \text{ N/m and } \tau = 0.9108 \text{ N/m}.$$

Figure 1 illustrates the size dependence in the non-dimensional natural frequency of TMB microbeams in comparison to classical solutions of TB. We can observe that for beam length on the order of nanometer to microns, the difference between natural frequencies is apparent and by increasing the length of the microbeam, the results tend to Timoshenko classical theory, that is, the surface effects are significant only in nanoscale. This same behavior was observed in (Abbasion et al., 2009) for a microbeam simply supported.

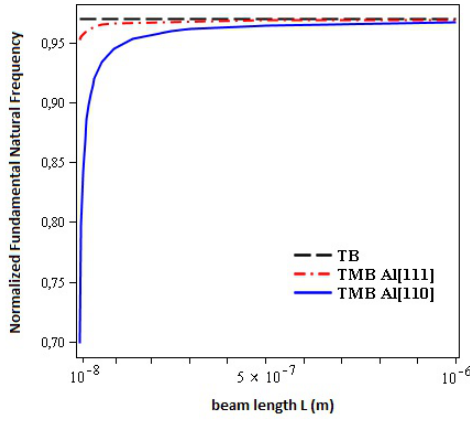


Figure 1: Influence of surface effects and size dependence on the normalized fundamental natural frequency of the microcantilever for $2h=0.2L$, $b=0.4L$ and $\kappa = 5/6$

3 Microcantilever beam with piezoelectric layer

A Timoshenko microcantilever beam actuated by a piezoelectric layer laminated on one side of the beam was studied in (Shirazi et al., 2012). The governing equations included viscous damping and the moment at the free end is subject to an applied voltage to piezoelectric layer. The equations and boundary conditions were established for a Timoshenko microcantilever with a laminated piezoelectric layer having length L , thickness h^p and width b as in Figure 2.

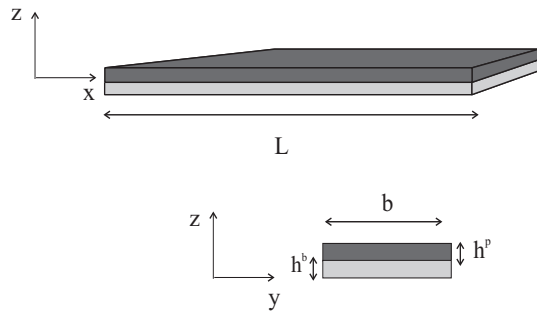


Figure 2: Schematic of beam with piezoelectric actuator

By incorporating the boundary condition due to piezoelectricity at the free end as a concentrated forcing into the model, we can describe this later as a forced damped Timoshenko microcantilever model. In matrix formulation, we have

$$M\ddot{\mathbf{v}} + C\dot{\mathbf{v}} + K\mathbf{v} = \mathbf{F}, \quad (24)$$

where

$$\mathbf{v} = \begin{pmatrix} w(t, x) \\ \psi(t, x) \end{pmatrix}, \quad \mathbf{F} = \begin{pmatrix} 0 \\ \frac{k_1}{D} \delta_1(x) V(t) \end{pmatrix},$$

$$\mathbf{M} = \begin{pmatrix} M_{11} & 0 \\ 0 & M_{22} \end{pmatrix}, \quad \mathbf{K} = \begin{pmatrix} K_{11} & K_{12} \\ K_{21} & K_{22} \end{pmatrix},$$

$$\mathbf{C} = \begin{pmatrix} c_1 & 0 \\ 0 & c_2 \end{pmatrix}. \quad (25)$$

Here

$$M_{11} = (\rho^p h^p b + \rho^b h^b b), \quad M_{22} = (\rho^p I^p + \rho^b I^b),$$

$$K_{11} = -4(\kappa'^p c_{55}^p h^p b + \kappa'^b c_{55}^b h^b b) \frac{\partial^2}{\partial x^2},$$

$$K_{12} = 4(\kappa'^p c_{55}^p h^p b + \kappa'^b c_{55}^b h^b b) \frac{\partial}{\partial x},$$

$$K_{21} = -4(\kappa'^p c_{55}^p h^p b + \kappa'^b c_{55}^b h^b b) \frac{\partial}{\partial x},$$

$$K_{22} = -(c_{11}^p I^p + c_{11}^b I^b) \frac{\partial^2}{\partial x^2} + 4(\kappa'^p c_{55}^p h^p b + \kappa'^b c_{55}^b h^b b),$$

$$k_1 = e_{13} z_m^p b, \quad u(t) = V(t), \quad D = c_{11}^p I^p + c_{11}^b I^b,$$

$$\kappa'^b = \frac{10(1+\nu^b)}{12+11\nu^b}, \quad \kappa'^p = \frac{10(1+\nu^p)}{12+11\nu^p}. \quad (26)$$

c_1 and c_2 are viscous damping constants, z_m is the distance between the middle line of the piezoelectric layer and the neutral axis of beam and $V(t)$ is the applied voltage to piezoelectric layer, $\delta_1(x)$ is the Dirac delta function applied at $x = L$.

4 AFM dynamic response

The dynamic response of the Timoshenko model (1) or equation (24) can be described in terms of the matrix impulse response or matrix Green function $\mathbf{h}(t, x, \xi)$ of the associated homogeneous initial-boundary value problem

$$M\ddot{\mathbf{h}}(t, x, \xi) + K\mathbf{h}(t, x, \xi) = \mathbf{0}, \quad 0 < x, \xi < L, \quad t > 0, \quad (27)$$

$$\mathbf{h}(0, x, \xi) = \mathbf{0}, \quad M\mathbf{h}_t(0, x, \xi) = \delta(x - \xi)\mathbf{I},$$

$$A\mathbf{h}(t, 0, \xi) + B\mathbf{h}_x(t, 0, \xi) = \mathbf{0},$$

$$P\mathbf{h}(t, L, \xi) + Q\mathbf{h}_x(t, L, \xi) = \mathbf{0},$$

where $\mathbf{0}$ denotes the 2×2 null matrix and \mathbf{I} the 2×2 identity matrix.

We have that $\mathbf{h}(t - \tau, x, \xi)$ acts as an integrating factor in Lagrange's adjoint method (Claeyssen et al., 2013). It turns out the dynamic response

$$\mathbf{v}(t, x) = \int_0^t \int_0^L (\mathbf{h}_t(\tau, x, \xi) M \mathbf{v}_0(\xi) + \mathbf{h}(\tau, x, \xi) M \mathbf{v}_1(\xi)) d\xi d\tau$$

$$+ \int_0^t \int_0^L \mathbf{h}(t - \tau, x, \xi) \mathbf{F}(\tau, \xi) d\xi d\tau + \mathbf{J}(\mathbf{v}, \mathbf{h})|_0^L, \quad (28)$$

where \mathbf{J} is a term containing effects of the initial-value Green function with values of \mathbf{v} at the boundary (Claeyssen et al., 2013).

4.1 Modal approximation of dynamic responses

The Galerkin method (Ginsberg, 2001) can be used for determining approximate dynamic responses of the AFM microcantilever beam described by the Timoshenko model. From (28), we actually need to find an approximation of the fundamental matrix response $\mathbf{h}(t, x, \xi)$. For this, we first introduce the block matrix

$$\mathbf{V}(x) = \begin{pmatrix} \mathbf{v}_1(x) & \mathbf{v}_2(x) & \dots & \mathbf{v}_n(x) \end{pmatrix}, \quad (29)$$

whose columns are the first n cantilever eigenfunctions (13) corresponding to the microcantilever eigenvalues, that have been normalized with respect to the mass matrix M . Then we consider obtaining an approximate response of the AFM microcantilever Timoshenko model (4)

$$\mathbf{v}(t, x) \doteq \sum_{j=1}^n p_j(t) \mathbf{v}_j(x) = \mathbf{V}(x) \mathbf{P}(t). \quad (30)$$

For determining the time amplitudes $\mathbf{P}^T(t) = \begin{pmatrix} p_1(t) & p_2(t) & \dots & p_n(t) \end{pmatrix}$ (Claeyssen et al., 2013), we have

$$\begin{aligned} \mathbf{v}(t, x) = & \int_0^L \mathbf{V}(x) \dot{\mathbf{h}}(t) \mathbf{V}^T(\mu) \mathbf{v}_o(\mu) d\mu + \\ & \int_0^L \mathbf{V}(x) \mathbf{h}(t) \mathbf{V}^T(\mu) \mathbf{v}_1(\mu) d\mu + \int_0^t \mathbf{V}(x) \mathbf{h}(t - \nu) \mathbf{V}^T(\mu) f d\nu. \end{aligned} \quad (31)$$

Consequently, we obtain the spectral approximation for the initial value Green matrix response

$$\mathbf{h}(t, \xi, \mu) \doteq \sum_{j=1}^N \frac{\sin(\omega_j t)}{\omega_j} \mathbf{v}_j(\xi) \mathbf{v}_j^T(\mu), \quad (32)$$

and for the transfer matrix function

$$\mathbf{H}(s, \xi, \mu) \doteq \sum_{j=1}^N \frac{\mathbf{v}_j(\xi) \mathbf{v}_j^T(\mu)}{s^2 + \omega_j^2}. \quad (33)$$

4.2 Results

The geometrical and material properties of the microbeam are described in Table 1. The first four obtained natural frequencies are shown in Table 2 for comparison with those of the formulated model in (Shirazi et al., 2012). The microcantilever shape matrix modes in Figure 3 are mass normalized. In Figure 4 is presented the displacement component of forced responses, considering spatial pulse moment excitations, that are modulated with a harmonic input $V(t)$ and with different spatial beam positions.

5 Conclusions

This work has addressed surface effects in AFM and tip-sample interaction with a microbeam built with smart materials. It was introduced a matrix formulation for those microbeams models that include rotatory inertia and shear deformations of

Properties of beam element		
Parameter(unit)	Symbol	Values
Length (μm)	L	150
Width (μm)	b	30
Thickness (μm)	h^b	10
Young Modulus (GPa)	c_{11}^b	73
Density (Kg/m^3)	ρ^b	2200
Poisson coefficient	ν^b	0.17
Properties of piezoelectric element		
Parameter(unit)	Symbol	Values
Length (μm)	l_p	150
Width (μm)	b	30
Thickness (μm)	h^p	10
Young Modulus (GPa)	c_{11}^p	71
Density (Kg/m^3)	ρ^p	7700
Poisson coefficient	ν^p	0.31

Table 1: Geometrical dimensions and material properties of beam and piezoelectric element

Freq. (KHz)	Reference (1)	Present work
1st	547	544
2nd	3314	3298
3rd	8833	8797
4th	15951	16210
(1): Reference (Shirazi et al., 2012)		

Table 2: Comparative natural frequencies

the Timoshenko model. This formulation has also been used with microbeams partially covered by piezoelectric materials leading to the study of multispan beams (Claeyssen et al., 2013).

The use of a fundamental matrix distributed response allows to determine modes and frequencies of microcantilevers and to predict forced responses. The eigenanalysis involves the task of solving a non-classical second-order damped differential equation whose stiffness matrix coefficient depends upon the frequency. It was observed that surface effects are significant only in nanoscale. Simulations with the forced piezoelectric microbeam model were performed by using the Galerkin method. The forced responses were computed when subject to pulse harmonic excitations at different positions.

Acknowledgments

The author L.Tonetto was supported by a doctoral fellowship from CAPES(Brazil).

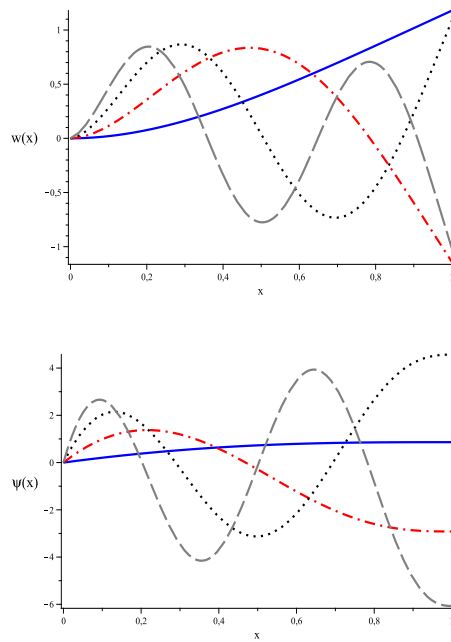


Figure 3: Mass normalized matrix shape modes of a microcantilever beam with a piezoelectric layer. Left: transversal deflection component $w(x)$. Right: rotation component $\psi(x)$. First mode: solid blue line, Second mode: dash-dotted red line, Third mode: dotted black line, Fourth mode: dashed gray line.

References

- Abbasion, S., Rafsanjani, A., Avazmohammadi, R. and Farshidianfar, A. (2009). Free vibration of microscaled Timoshenko beam, *Applied Physics Letters* **95**(14): 143122. DOI: [10.1063/1.3246143](https://doi.org/10.1063/1.3246143)
- Claeyssen, J. and Costa, S. (2006). Modes for the coupled Timoshenko model with a restrained end, *Journal of Sound and Vibration* **296**(4-5): 1053–1058.
- Claeyssen, J. R., Canahualpa, G. and Jung, C. (1999). A direct approach to second-order matrix non-classical vibrating equations, *Applied Numerical Mathematics* **30**(1): 65–78. DOI: [10.1016/S0168-9274\(98\)00085-3](https://doi.org/10.1016/S0168-9274(98)00085-3)
- Claeyssen, J., Tsukazan, T., Tonetto, L. and Tolfo, D. (2013). Modeling the tip-sample interaction in atomic force microscopy with Timoshenko beam theory, *Journal of Sound and Vibration* (2) DOI: [10.2478/nsmm-2013-0008](https://doi.org/10.2478/nsmm-2013-0008)
- Eslami, S. and Jalili, N. (2012). A comprehensive modeling and vibration analysis of afm microcantilevers subjected to nonlinear tip-sample interaction forces, *Ultramicroscopy* **117**: 31–45. doi: [10.1016/j.ultramic.2012.03.016](https://doi.org/10.1016/j.ultramic.2012.03.016)
- Ginsberg, J. (2001). *Mechanical and Structural Vibrations*, John Wiley.

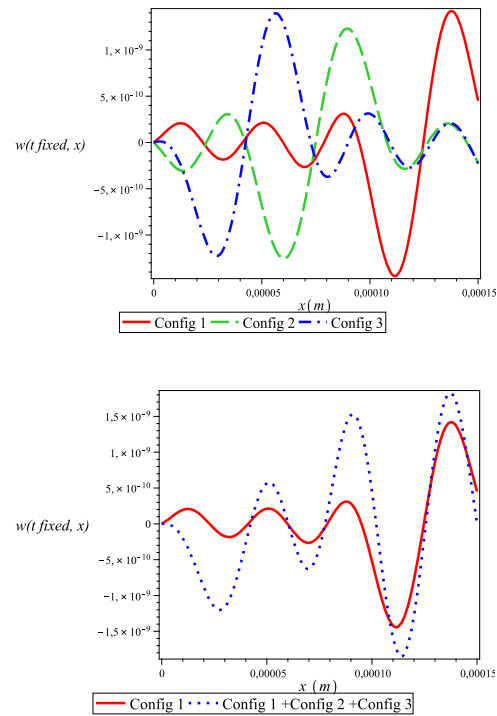


Figure 4: Above: transversal deflection component $w(t, x)$, with $t = 3 \times 10^{-9}$, due to a different rectangular pulse moment **Config 1**: $k_1/D(H(x-7L/9)-H(x-8L/9))V(t)$, **Config 2**: $k_1/D(H(x-4L/9)-H(x-5L/9))V(t)$. **Config 3**: $k_1/D(H(x-2L/9)-H(x-3L/9))V(t)$. Below: Comparative $w(t, x)$, with $t = 3 \times 10^{-9}$, due to a combined effects of previous pulses.

- Gurtin, M., Weissmuller, J. and Larche, F. (1998). A general theory of curved deformable interfaces in solids at equilibrium, *Philosophical Magazine A* **75**(5): 1093–1109. DOI: [10.1080/01418619808239977](https://doi.org/10.1080/01418619808239977)
- Hsu, J., Lee, H. L. and Chang, W. (2007). Flexural vibration frequency of atomic force microscope cantilevers using the Timoshenko beam model, *Nanotechnology* **18**: 28503–28508. DOI: [10.1088/0957-4484/18/28/285503](https://doi.org/10.1088/0957-4484/18/28/285503)
- Jalili, N. (2010). *Piezoelectric-Based Vibration Control: From Macro to Micro/Nano Scale Systems*, Springer-Verlag. DOI: [10.1007/978-1-4419-0070-8](https://doi.org/10.1007/978-1-4419-0070-8)
- Laxminarayana, K. and Jalili, N. (2004). A review of atomic force microscopy imaging systems: application to molecular metrology and biological sciences, *Mechatronics* **14**: 907–945. DOI: [10.1016/j.mechatronics.2004.04.005](https://doi.org/10.1016/j.mechatronics.2004.04.005)
- Shirazi, M., Salarieh, H., Alasty, A. and Shabani, R. (2012). Tip tracking control of a microcantilever Timoshenko beam via piezoelectric actuator, *Journal of Vibration and Control* **117**: 1–14.
- Wang, G. and Feng, X. (2007). Effects of surface elasticity and residual surface tension on the natural frequency of microbeams, *Applied Physics Letters* **90**: 231904. DOI: [10.1063/1.2746950](https://doi.org/10.1063/1.2746950)